ISSN 1392–1320 MATERIALS SCIENCE (MEDŽIAGOTYRA). Vol. 21, No. 4. 2015

Inhibition Effect of N, N'-Dimethylaminoethanol on the Pitting Corrosion Austenitic Stainless Steel Type 304

Roland Tolulope LOTO [1, 2]*, Cleophas Akintoye LOTO [1, 2], Patricia Abimbola POPOOLA [2], Tatiana FEDOTOVA [2]

[1] *Department of Mechanical Engineering, Covenant University, Ota, Ogun State, Nigeria*
[2] *Department of Chemical, Metallurgical & Materials Engineering, Tshwane University of Technology, Pretoria, South Africa*

crossref http://dx.doi.org/10.5755/j01.ms.21.4.8977

Received 22 December 2014; accepted 17 May 2015

The electrochemical influence and corrosion inhibition of N, N'-dimethylaminoethanol on the pitting corrosion resistance of austenitic stainless steel (type 304) in dilute sulphuric acid solution with sodium chloride addition was investigated using potentiodynamic polarization technique. Corrosion potential, pitting potential, passivation potential, nucleation resistance, passivation range and repassivation capacity measurements and potentiodynamic analysis were used to evaluate the steel's pitting resistance characteristics. The potentiodynamic experiments revealed that pitting potential increased with increase in concentration of the inhibiting compound coupled with an increase in the passivation range hence increased resistance to pitting corrosion.
Keywords: corrosion, n, n'-dimethylaminoethanol, pitting, inhibition.

1. INTRODUCTION

Austenitic stainless steels have unusual corrosion resistance and exceptional mechanical properties which enable versatile applications cutting across numerous industries such as heat exchanger systems, drilling platforms, wastewater treatment, desalination plants etc. as a result of its long service life with low maintenance cost, recyclability, harmless effect on the environment and human health, adequate high temperature mechanical properties, good fabricability and weldability. The superior corrosion resistance of stainless steel is due to a naturally formed adherent and compact flawless oxide film on the surface. In aqueous medium the passive film formed on the stainless steel is duplex in nature, consisting of a chromium-rich inner barrier oxide layer and iron-rich outer deposited hydroxide or salt layer [1 – 10]. Despite these stainless steels are susceptible to localized breakdown on the surface, at the site of defects in the presence of aggressive chloride ions. This results in pitting corrosion and severe damage to the structure [11].

Pitting corrosion is a localized electrochemical dissolution process, which under some circumstances results in catastrophic failure of the stainless steel. This form of localized corrosion attack occurs on small areas of the metal surface, while the remaining surface remains unaffected. Pitting is particularly insidious in nature due to the extent of rapidly and penetrates into the mass of the extent of rapidly and penetrates into the mass of the metal.

The result of the rapid perforation of thin metal sections can induce leakage of fluid or alternatively, pitting to crack transition may occur with consequential crack nucleation and growth which leads to brittleness and catastrophic failure [12, 13]. The location of pits on metals that develop passive films is often unpredictable with pits tending to randomly disperse on the metal surface, though there is evidence for preferential location at non-metallic inclusions [14 – 17]. The initial event in localized corrosion of stainless steels is passivity breakdown, followed by pit nucleation, growth, and in some cases repassivation in corrosion resistant metals in aqueous solutions [18, 19].

This study aims to investigate the corrosion inhibition effect of N, N'-dimethylethanolamine an amino alcohol compound and its ability to provide protection against pitting corrosion at specific concentrations in 3 M H_2SO_4 test solutions using linear polarization technique.

2. EXPERIMENTAL PROCEDURE

2.1. Material

Type 304 austenitic stainless steel was analyzed at the Electrochemical & Materials Characterization Laboratory, Tshwane University of Technology, South Africa. The steel has the nominal per cent composition of 18.11 % Cr, 8.32 % Ni and 68.32 % Fe.

2.2. Inhibitor

N, N'-Dimethylaminoethanol (DMAE) a colorless, transparent liquid is the inhibitor used. The structural formula of DMAE is shown in Fig. 1. The molecular formula is $C_4H_{11}NO$ while the molar mass is 89.14 g mol^{-1}.

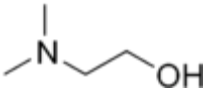

Fig. 1. Chemical structure of N, N dimethylaminoethanol (DMAE)

DMAE was prepared in concentrations of 2.5 %, 5 %, 7.5 %, 10 %, 12.5 % and 15 %.

* Corresponding author. Tel.: +2348084283392.
E-mail address: *tolu@gmail.com* (R.T. Loto)

2.3. Test media

3M tetraoxosulphate (VI) acid with 3.5 % recrystallized sodium chloride of Analar grade was used as the corrosion test media.

2.4. Preparation of test specimens

The cylindrical stainless steel specimens were mechanically cut into a number of test specimens of dimensions in length ranging from 17.8 mm and 18.8 mm coupons. The two surface ends of each of the specimen were ground with silicon carbide abrasive papers of 80, 120, 220, 800 and 1000 grits. They were then polished with 6.0 µm to 1.0 µm diamond paste, washed with distilled water, rinsed with acetone, dried and stored in a desiccator for further weight-loss test and linear polarization.

2.5. Linear polarization resistance

Linear polarization measurements were carried out using, a cylindrical coupon embedded in resin plastic mounts with exposed surface of 254 mm^2. The electrode was polished with different grades of silicon carbide paper, polished to 6 µm, rinsed by distilled water and dried with acetone. The studies were performed at ambient temperature of 25 °C with Autolab PGSTAT 30 ECO CHIMIE potentiostat and electrode cell containing 200 ml of electrolyte, with and without DMAE inhibitor. A graphite rod was used as the auxiliary electrode and silver chloride electrode (Ag/AgCl) was used as the reference electrode. The steady state open circuit potential (OCP) was noted. The potentiodynamic studies were made from - 1.5 V *versus* OCP to + 1.5 V *versus* OCP at a scan rate of 0.00166 V/s and the corrosion currents were registered. The corrosion current density (j_{cr}) and corrosion potential (E_{cr}) were determined from the Tafel plots of potential *versus* log *I*. The corrosion rate (*R*), the degree of surface coverage (θ) and the percentage inhibition efficiency (%*IE*) were calculated as follows

$$R = \frac{0.00327 \; x \; icorr \; x \; E_q}{D}, \quad (1)$$

where i_{cr} is the current density in µA/cm^2. *D* is the density in g/cm^3 while E_q is the specimen equivalent weight in grams. The percentage inhibition efficiency (%*IE*) was calculated from corrosion current density values using the equation.

$$\%IE = 1 - \left[\frac{R_2}{R_1}\right] \cdot 100, \quad (2)$$

where $R_1$and R_2 are the corrosion current densities in absence and presence of inhibitors, respectively.

3. RESULTS AND DISCUSSION

3.1. Polarization studies

Potentiostatic potential was cursorily examined from -1.5 to + 1.5 V vs. Ag/AgCl at a rate of 0.0166 mV s^{-1}, which allows for quasi-stationary state measurements. Fig. 2 a and b shows the polarization curves of the stainless steel in absence and presence of DMAE at specific concentrations in 3M H_2SO_4 solution.

Increase in DMAE concentration results in progressive increase in inhibition efficiency of DMAE compound due to the inhibiting action of DMAE molecules in counteracting the electrochemical actions of the corrosive anions and stifling the active sites through formation of an impenetrable barrier film on the alloy surface in the acid solutions. Linear polarization results show that adsorbed DMAE compound restricts the electrochemical process of corrosion on the steel surface. The electrochemical current parameter was significantly influenced due to increase in DMAE concentrations.

Generally, the scans in Fig. 2 a and b depict slightly similar behavior over the potential domain. There was a drastic reduction in corrosion rate but the electrochemical parameters varied differentially with DMAE addition. This shows that DMAE significantly alters the electrochemical reactions responsible for corrosion degradation. Additionally, changes in the cathodic and anodic Tafel constants signify that the redox electrochemical reactions are slowed down by the surface blocking effect of the inhibitor. The corrosion inhibition property of DMAE is directly related to its adsorption on the electrode surface. Electrochemical variables such as, corrosion potential (E_{cr}), corrosion current (i_{cr}) corrosion current density (I_{cr}), cathodic Tafel constant (*bc*), anodic Tafel slope (*ba*), surface coverage θ and percentage inhibition efficiency (%*IE*) were calculated and given in Table 1. The corrosion current density (I_{cr}) and corrosion potential (E_{cr}) were determined by the intersection of the extrapolating anodic and cathodic Tafel lines.

Observation of Table 1 shows DMAE compound act as a mixed type inhibitor in the 3M H_2SO_4 solution. The redox electrochemical reactions were influenced by the presence of DMAE in the acid media, with greater effect on the anodic electrochemical reactions which generally involves metal breakdown and dissolution in the presence of corrosive ions.

Table 1. Data obtained from polarization resistance measurements for austenitic stainless steel in 3M H_2SO_4/DMAE concentrations

Inhibitor concentration, %	Corrosion rate, mm/yr	%, *IE*	R_p, Ω	E_{cr}, Obs, V	E_{cr}, Cal, V	i_{cr}, A	I_{cr}, A/cm^2	*bc*, V/dec	*ba* , V/dec
0	8	0	4.58	-0.328	-0.036	1.78E-03	7.01E-04	0.026	0.067
2.5	2.77	65.42	16.3	-0.263	-0.811	6.17E-04	2.43E-04	0.21	0.026
5	2.07	74.06	41.65	-0.263	-0.612	4.61E-04	1.81E-04	0.185	0.058
7.5	1.56	80.54	38.42	-0.291	0.028	3.47E-04	1.37E-04	0.207	0.036
10	1.24	84.48	59.46	-0.308	-0.748	2.76E-04	1.09E-04	0.064	0.092
12.5	1.05	86.85	58.61	-0.319	-0.807	2.34E-04	9.21E-05	0.092	0.048
15	1.03	87.46	60.00	-0.374	-0.118	2.29E-04	9.02E-05	0.049	0.089

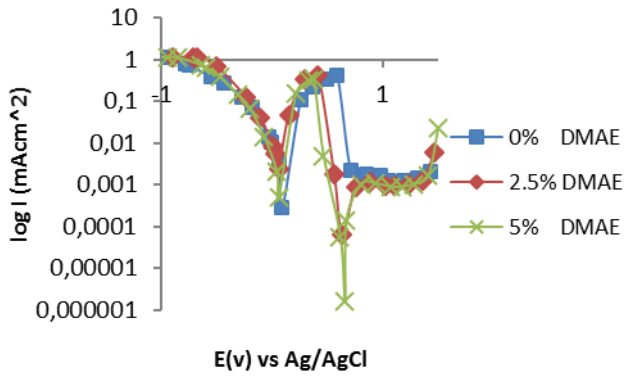

a

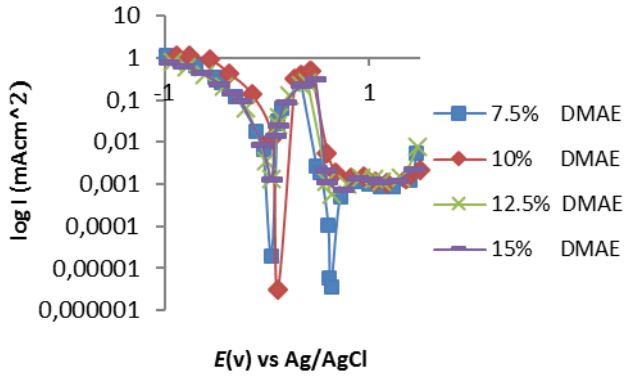

b

Fig. 2. Comparison plot of cathodic and anodic polarization scans for austenitic stainless steel in 3 M H_2SO_4 + 3.5 % NaCl solution at specific concentrations of DMAE: a – 0 % – 5 % DMAE; b – 7.5 % – 15% DMAE

When compared to the cathodic reactions which involve hydrogen evolution and oxygen reduction reactions, the nitrogen atoms within the molecule of DMAE protonates in the acid solution before electrostatic adsorption on the metal surface [20]. Moreover, the presence of the hydroxyl group in the compound increased its solubility in the electrolytic media thereby enhancing the corrosion inhibition process. The increase in the number of adsorbed DMAE molecules on the steel is proportional to increase in the percentage increase in DMAE concentration. This mechanism obstructs the electrolytic transport of ionic species (chlorides and sulphates) from the electrode surface as the surface coverage value (θ) increases. The adsorption blocks the reaction sites of the metal surface thus affecting the anodic reaction mechanism.

Corrosion potentials slightly shifts in the positive direction in with a maximum displacement in E_{cr} value of 54 mV in H_2SO_4, thus in H_2SO_4 DMAE showed mixed inhibiting characteristics. Small alteration in corrosion potentials is most probably as a result of competition between the anodic and the cathodic electrochemical inhibiting reactions. In Fig. 2 a, b the current density starts to increase very steeply due to active metal dissolution reaction, then stabilizes over a passivation zone extending to ~1000 mV indicating strong resistance to pitting corrosion before it starts again to increase faster due to breakdown of the passive film and pit initiation.

The values of the anodic Tafel slope can be attributed to both surface kinetic process and diffusion control, where the inhibitor molecules are adsorbed via their reactive functional groups on to the steel surface forming an impenetrable protective layer over the metal surface thus preventing the electrolytic transport of sulphate and chloride anions. Furthermore, the results in Table 1 demonstrate clearly the inhibitory effect of DMAE on the stainless steel corrosion whereby both i_{cr} and corrosion rate decreases, accompanied by a decrease in polarization resistance (R_p). The inhibition mechanism of DMAE compounds is a combination of surface blockage and electrostatic repulsion between adsorbed species and corrosive anions.

3.2. Nucleation resistance, passivation capacity, passivation range and passivation potential

The pit nucleation resistance NR ($E_{pit} - E_{cr}$), passivation range ($E_{pit} - E_{pp}$) and passivation capacity PC ($E_{pp} - E_{cr}$) can be considered to be a measure of the susceptibility of alloys to pitting corrosion [21]. Alloys exhibiting higher values of nucleation resistance and lower values of repassivation capacity are more resistant to pitting corrosion. The values of NR and PC are shown in Table 2. Nucleation occurrence is the product of the creation and evolution of metastable pits. These pit forms and develop for short period before passivation, at potentials well beneath the pitting potential and during the induction time before the onset of stable pitting at potentials above the pitting potential. Nucleations symbolize the breakdown and repassivation of the passive film and occur extremely rapidly. Current increase depicts the initiation and progression of pits while the instantaneous decrease represents repassivation and pit termination. Specific accumulation of chloride complexes results in the formation of meta-soluble precipitate on the metal surface [16]. This hampers the stability of the passive film at lower to higher potentials. The sequential hysteries in current value depict the sequential breakage and formation of occlusions during metastability which increases the porosity of the covering. The difference between NR and CR for the polarization curves shows the passivation range on the table (region B-J).

3.3. Influence of DMAE on the pitting corrosion evaluation of austenitic stainless steel in 3M H_2SO_4

Detailed observation of Fig. 3 b, d shows that increase in DMAE concentration causes a sharp increase in the metastable region of the polarization curve; there is a continuous increase of that portion before gradual decrease in Fig. 3 d. This illustration emphasizes the electrochemical influence of DMAE at low concentrations. At this portion even though the overall impact is positive due to reduced corrosion rate (Table 2) DMAE delays the early formation of the passive film necessary for the structural stability of surface properties of the steel. At Fig. 3 e – g there is a sharp decrease of the metastable region due to the influence of DMAE at high concentrations and the swift formation of chromium oxide on the steel alloy, thus the system attains stable passivation early. At low concentrations DMAE delays the onset of

passivation but its overall influence on the passive region is insignificant as shown in the slight increase in the passivation potential range values.

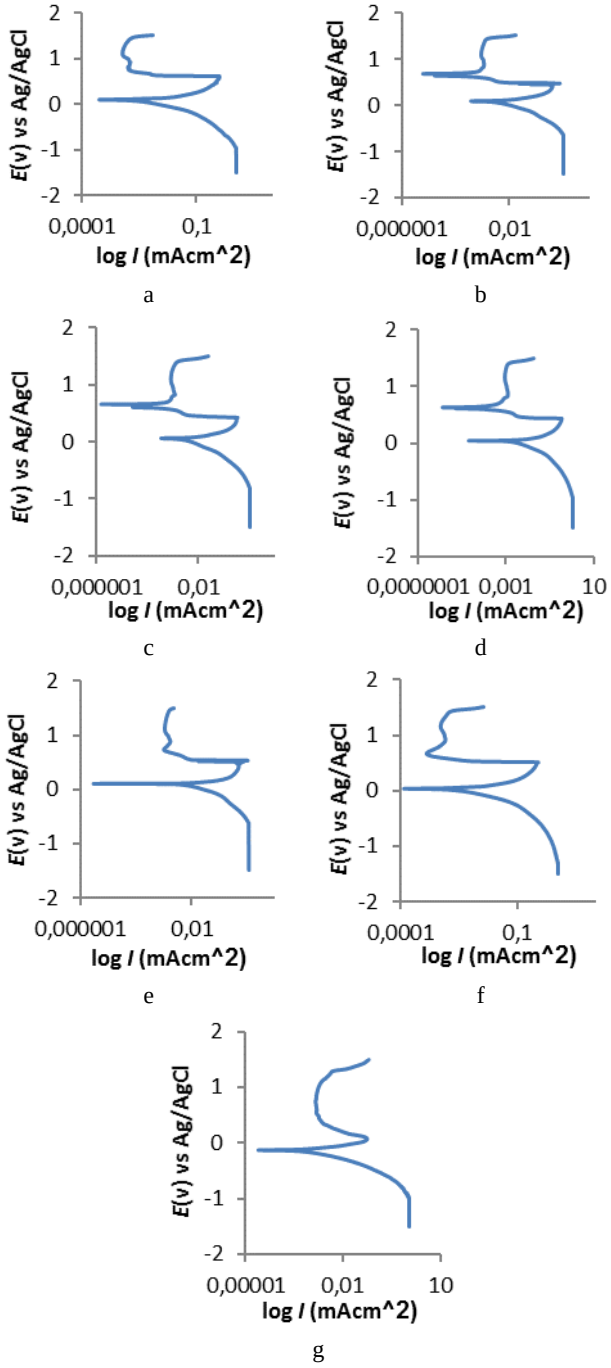

Fig. 3. Polarization curve of ASS in 3M H2SO4 solution at specific concentrations of DMAE (0 % – 15 % DMAE)

This further confirms the inhibiting effect of DMAE in 3M H_2SO_4 is more of surface film formation which separates the active sites on the alloys from the chloride and sulphate ions. These ions significantly aggravate the conditions for formation and growth of the pits in region P-Q, the region at which the anodic polarization exceeds the critical pit initiation potential (E_{pit}- pitting potential) due to anodic dissociation. The film-breaking and adsorption mechanism of pit formation best explains the electrolytic activity. The process starts with cracks in the DMAE film/passive layer exposing small areas of bare metal surface to the electrolyte. This causes the transfer of cations to the electrolyte due to the action of aggressive anions which also diffuses into the alloy through an autocatalytic process. This process causes a thinning and final removal of DMAE film, thus exposing the bare metal surface to further corrosion. During upward scanning, breakdown occurs at point Q and a stable pit starts to grow. During this stage, active dissolution of the metal matrix takes place continuously in the pit.

The pitting potential values (E_{pit}), for austenitic stainless steel in 3 M H_2SO4 is shown in Table 2. The E_{pit} value increased with increase in DMAE concentration from sample A to F. At sample G there was a slight decrease in the pitting potential, however this value was upset by the passivation potential and passivation range values (Table 2) due to the action of DMAE molecules. At this concentration, the steel sample showed a relative tendency to quickly passivate at lower potentials coupled with high corrosion resistance. Secondly its passivation range is the widest i.e. it's able to maintain its passive state for longer periods. The same goes for other concentrations because with the addition of DMAE at all concentrations the passivation range values increases progressively; the passivation potential becomes nobler and the passivation capacity values declines. These values are an indication of the inhibitive effect of DMAE on the electrochemical reactions taking place on the microstructure of the stainless steel specimen.

The values of E_{pit} illustrate the inhibition performance of DMAE in delaying the formation of pits under induced corrosion. Pitting occurred at a higher potential due to the reduced influence of chloride and sulphate ions by DMEA adsorption onto the metal oxide. At E_{pit}, the initiation of pitting could be ascribed to competitive adsorption between SO_4^{2-}/Cl^- ions due to breakage or chemical modification of the protective film at high potentials [22, 23].

Table 2. Potentiostatic values ASS in 3M H_2SO_4 solution/DMAE

Sample	Inhibitor conc., C	Pitting potential, v	Passivation potential, v	Passivation range, v	Nucleation resistance, v	Repassivation capacity, v
A	0	1.317	0.707	0.61	1.645	1.035
B	0.00028	1.376	0.668	0.708	1.619	0.911
C	0.00056	1.38	0.658	0.684	1.643	0.921
D	0.00084	1.386	0.634	0.752	1.703	0.925
E	0.00112	1.425	0.629	0.845	1.773	0.937
F	0.0014	1.429	0.609	0.811	1.793	0.928
G	0.00168	1.308	-0.343	0.967	1.672	0.031

The SO_4^{2-}/Cl^- ions displace the adsorbed DMAE anions at some locations, thus penetrating it under high electric field across the film and accelerate localized anodic dissolution. Increase in DMAE concentration shifts the value of E_{pit} to more positive potentials commensurate with an increase in the alloy resistance to corrosion. The passivation potentials depict the relative capacity of the alloy.

Acknowledgements

The authors acknowledge the department of Chemical, Metallurgical and Materials Engineering, Faculty of Engineering and the Built Environment, Tshwane University of Technology, Pretoria, South Africa for the provision of research facilities for this work.

REFERENCES

1. **Ramana, K.V.S., Anita, T. S., Mandal, S., Kaliappan, S., Shaikh, H., Sivaprasad, P.V., Dayal, R.K., Khatak, H.S.** Effect of different Environmental Parameters on Pitting Behavior of AISI Type 316L Stainless Steel: Experimental Studies and Neural Network Modeling *Materials & Design* 30 2009: pp. 3770 – 3775.
2. **Ramya, S., Anita, T., Shaikh, H., Dayal, R. K.** Laser Raman Microscopic Studies of Passive Films formed on Type 316LN Stainless Steels during Pitting in Chloride Solution *Corrosion Science* 52 2010: pp. 2114 – 2121.
3. **Almarshad, A.I, Jamal, D.** Electrochemical Investigations of Pitting Corrosion Behaviour of Type UNS S31603 Stainless Steel in Thiosulfate-Chloride Environment *Journal of Appllied Electrochem*istry 34 2004: pp. 67 – 70.
4. **Nakayama, T., Oshida, Y.** Identification of the Initial Oxide Films on 18-8 Stainless Steel in High Temperature Water *Corrosion Journal* 24 1968: pp. 336 – 337.
5. **Schweitzer, P.A.** Encyclopaedia of Corrosion Technology, 2nd ed., CRC Press, USA, 432 2004. http://dx.doi.org/10.1201/9780824750442
6. **Schweitzer, P.A.** Metallic Materials: Physical, Mechanical, and Corrosion Properties, 1st ed. CRC Press, USA, 36 2003. http://dx.doi.org/10.1201/9780203912423
7. **Kudo, K.T., Shibata, G., Okamoto, G., Sato, N.** Ellipsometric and Radiotracer Measurements of the Passive Oxide Film on Fe in Neutral Solution *Corrosion Science* 8 1968: pp. 809 – 814.
8. **Okamoto, G.** Passive Film of 18-8 Stainless Steel Structure and its Function *Corrosion Science* 13 1973: pp.471 – 489. http://dx.doi.org/10.1016/0010-938X(73)90031-0
9. **Galvele, J.R.** Transport Processes in Passivity Breakdown—II. Full hydrolysis of the Metal Ions *Corrosion Science* 21 1981: pp. 551 – 579.
10. Standard Guide G48-92, *Annual Book of ASTM Standards*, Philadelphia PA, ASTM, 1994: pp. 652.
11. **Fossati, A., Borgioli, F., Galvanetto, E., Bacci, T.** Corrosion Resistance Properties of Glow-Discharge Nitrided AISI 316L Austenitic Stainless Steel in NaCl Solutions *Corrosion Science* 48 2006: 1513 – 1527. http://dx.doi.org/10.1016/j.corsci.2005.06.006
12. **Turnbull, A., McCartney, L.N., Zhou, S.** A Model to Predict the Evolution of Pitting Corrosion and the Pit-to-Crack Transition Incorporating Statistically Distributed Input Parameters *Corrosion Science* 48 2006: pp.2084 – 2105. http://dx.doi.org/10.1016/j.corsci.2005.08.010
13. **Kondo, Y.** Prediction of Fatigue Crack Initiation Life Based on Pit Growth *Corrosion Journal* 45 1989: pp. 7 – 11.
14. **Isaacs, H.S.** The Localized Breakdown and Repair of Passive Surfaces during Pitting *Corrosion Science* 29 1989: pp. 313 – 323. http://dx.doi.org/10.1016/0010-938X(89)90038-3
15. **Macdonald, D.D.** Point Defect Model for the Passive State *Journal of Electrochemical Science* 13 (12) 1992: pp. 3434 – 3449.
16. **Burstein, G.T., Liu, C., Souto, R.M., Vines, S.P.** Origins of Pitting Corrosion *Corrosion Engineering Science and Technology* 39 (10) 2004: pp. 25 – 30. http://dx.doi.org/10.1179/147842204225016859
17. **Djoudjou, R., Lemaitre, C., Beranger, G.** Role of Sulphide Inclusions on the Pitting of Stainless Steel in Chloride Media *Corrosion Reviews* XI (3/4) 1993: pp. 157 – 176.
18. **Burstein, G.T., Pistorius, P.C., Mattin, S.P.** The Nucleation and Growth of Corrosion Pits on Stainless Steel *Corrosion Science* 35 (1 – 4) 1993: pp. 57 – 62.
19. **Pistorius, P.C., Burstein, G.T.** Detailed Investigation of Current Transients from Metastable Pitting Events on Stainless Steel –The Transition to Stability *Materials Science Forum* 111 – 112 1992: pp. 429 – 452.
20. **Peng, Z., Cheng, Z., Lei, Hunag, L.N., Fushi, Z.** Corrosion Inhibition of Dibenzo [1, 4, 8, 11] Tetraaza [14] Annulene Nickel on Steel in 1 M HCl *Corrosion Science* 50 (8) 2008: pp. 2166 – 2171. http://dx.doi.org/10.1016/j.corsci.2008.06.015
21. **Ajit, K.M., Balasubramaniam, R.** Corrosion Inhibition of Aluminium by Rare Earth Chlorides *Materials Chemistry and Physics* 103 (2 – 3) 2007: pp. 385 – 393.
22. **Kolics, A., Polkinghorne, J.C., Wieckowski, A.** Adsorption of Sulfate and Chloride Ions on Aluminum *Electrochimica Acta* 43 (18) 1998: pp. 2605 – 2618.
23. **Ming-Yu, C., Ge-Ping, Yu.** Pitting Corrosion of Inconel 600 in Chloride and Sulfate Solutions at Low Temperature *Journal of Nuclear Materials* 202 (1 – 2) 1993: pp. 145 – 153.